

On the Structure and Stability of Gas-Phase Cluster Ions $\text{SiF}_3^+(\text{CO})_n$, $\text{SiF}_3\text{OH}_2^+(\text{SiF}_4)_n$, $\text{SiF}_4\text{H}^+(\text{SiF}_4)_n$, and $\text{F}^-(\text{SiF}_4)_n$

Kenzo Hiraoka,* Masayuki Nasu, Akihito Minamitsu, and Akitaka Shimizu

Faculty of Engineering, Yamanashi University, Takeda-4, Kofu 400-8511, Japan

Shinichi Yamabe*

Department of Chemistry, Nara University of Education, Takabatake-cho, Nara 630-8528, Japan

Received: February 9, 2000; In Final Form: April 27, 2000

Gas-phase ion/molecule reactions in SiF_4 were measured using a pulsed-electron beam mass spectrometer. The thermochemical stabilities of $\text{SiF}_3^+(\text{CO})_n$, $\text{SiF}_3\text{OH}_2^+(\text{SiF}_4)_n$, $\text{SiF}_4\text{H}^+(\text{SiF}_4)_n$, and $\text{F}^-(\text{SiF}_4)_n$ have been studied experimentally and theoretically. Owing to the serious charging of the ion source, only up to $n = 2$ thermochemical data could be obtained experimentally. The bond energy for $\text{SiF}_3^+\cdots\text{CO}$ of 41.6 kcal/mol is found to be much larger than that for $\text{CF}_3^+\cdots\text{CO}$ of 16.0 kcal/mol. This indicates that SiF_3^+ is a much stronger Lewis acid than CF_3^+ . The $\text{SiF}_3^+(\text{CO})_2$ cluster has the D_{3h} structure, $\text{OC}\cdots\text{SiF}_3^+\cdots\text{CO}$, which is the core for the larger cluster ions, $[\text{SiF}_3(\text{CO})_2]^+(\text{CO})_{n-2}$. In the cluster ion $\text{SiF}_4\text{H}^+(\text{SiF}_4)_2$, a C_2 symmetry structure, $(\text{F}_3\text{-Si}\cdots\text{F-H-F}\cdots\text{SiF}_3)^+$, has been obtained. In the cluster $\text{F}^-(\text{SiF}_4)_2$, the F^- ion is sandwiched by the two SiF_4 molecules equivalently, indicating the charge dispersal in the complex.

1. Introduction

Silane and its halo derivatives have received considerable attention because of their importance in the semiconductor industry. The chemical properties of ionic and neutral species are fundamental to the understanding of processes such as chemical vapor deposition (CVD), glow discharge deposition, and plasma etching.¹ In particular, silicon fluoride has been extensively studied^{2–10} because it is used to etch and deposit silicon layers in the fabrication of microelectronics devices and solar cells.

Armentrout et al. studied the thermochemistry of SiF_x^+ using a guided ion beam mass spectrometer.^{2,3} Gutsev calculated the electronic and geometrical structure of the ground and low lying excited states of the SiF_n and SiF_n^- series ($n = 1–5$) within a local spin density approximation augmented with the nonlocal gradient corrections to the exchange functional.⁴ Jacox et al. measured the infrared spectra of SiF_3^+ and SiF_3^- by the matrix isolation method.⁵ Schaeffer, III, et al. employed density functional methods to determine the molecular structures and total energies of SiF_n and SiF_n^- ($n = 1–5$).⁶ They predicted that the SiF_3^- anion is more strongly pyramidal than SiF_3 . Hiraoka et al. made experimental and theoretical studies of gas-phase ion/molecule reactions in SiF_4 and determined the thermochemical stabilities of $\text{SiF}_m^+(\text{SiF}_4)_n$ clusters ($m = 0–3$ and $n = 0–2$).⁷ However, the association ability of ions derived from SiF_4 needs to be examined more extensively.

In this work, as a challenge to species which are extremely difficult to deal with, thermochemical stabilities of gas-phase cluster ions $\text{SiF}_3^+(\text{CO})_n$, $\text{SiF}_3\text{OH}_2^+(\text{SiF}_4)_n$, $\text{SiF}_4\text{H}^+(\text{SiF}_4)_n$, and $\text{F}^-(\text{SiF}_4)_n$ have been studied. A characteristic difference in the bonding nature between the isovalent SiF_3^+ and CF_3^+ has been observed.

2. Experimental and Computational Method

The experiment was performed with a pulsed electron beam high-pressure mass spectrometer.^{11,12} In the SiF_4/CO or SiF_4/H_2 system, a small amount of SiF_4 (0.1–0.5 Torr) was introduced into the ~ 3 Torr major gas (CO or H_2) through a stainless steel capillary (1 mm long \times 0.1 mm in diameter). In the measurement for the clustering reaction of F^- with SiF_4 , ~ 0.1 Torr of F^- -forming NF_3 reagent gas was fed into the ~ 3 Torr major $\text{He}/\text{SiF}_4(95/5)$ gas through a stainless steel capillary (1 m long \times 0.1 mm in diameter). The ions escaping from the field-free ion source into an evacuated region were mass analyzed by a quadrupole mass spectrometer (ULVAC, MSQ-400, $m/z = 1–550$).

In this experiment, a serious decrease in the ion signals was observed with a decrease of ion source temperature. This was due to the charging of the surface of the ion source. As is known that SiF_4 is used as a reagent gas for fabrication of polycrystalline silicon by plasma-enhanced chemical vapor deposition, the charging may be due to a thin solid film formed on the surface of the ion source. It was found that the observed charging effect was moderately suppressed when the surface of the ion source was coated with colloidal graphite. All the experimental data presented here were obtained using the graphite-coated ion exit slit. Due to the weak signal intensities, great care must be taken to obtain reliable thermochemical data.

Geometries of $\text{SiF}_3^+(\text{CO})_n$, $\text{SiF}_3\text{OH}_2^+(\text{SiF}_4)_n$, and $\text{SiF}_4\text{H}^+(\text{SiF}_4)_n$ ($n = 0, 1$, and 2) were optimized by a Becke3LYP/6-31G* method.¹³ Possible structural isomers were sought and stable ones were picked up. The most stable isomer is (a), and the next one is (b) when it exists. Subsequent vibrational analyses were made to check whether the geometries obtained are correctly located at their stable points and to obtain zero-point vibrational energies (ZPEs). For $\text{SiF}_3^+(\text{CO})_1$, $\text{SiF}_3\text{OH}_2^+$ -

* Corresponding authors.

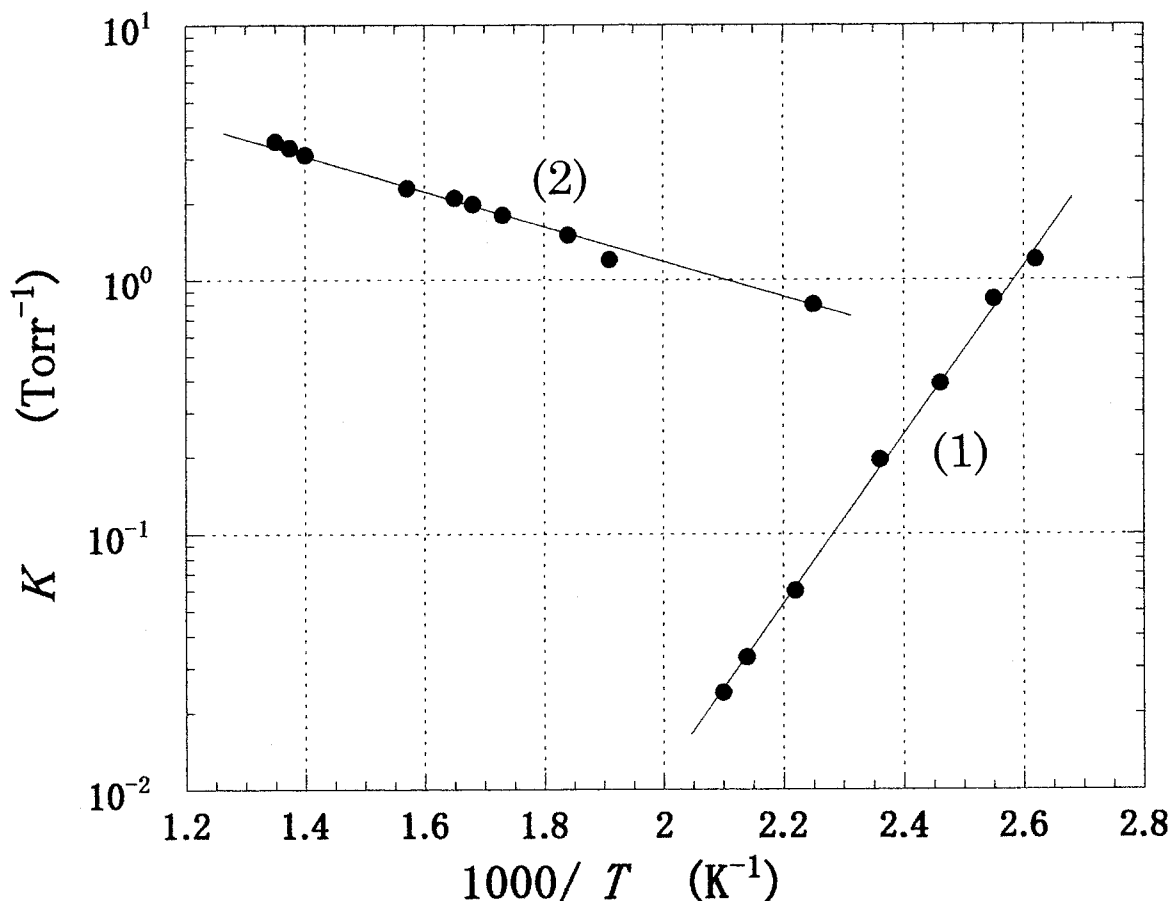
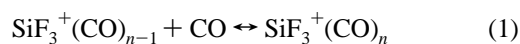


Figure 1. van't Hoff plots for equilibria for clustering reaction 1 with $n = 2$, and displacement reaction 2.

(SiF₄)₀, and SiF₄H⁺(SiF₄)₀, Si⋯C, Si⋯O, and Si⋯F distances were calculated by B3LYP with five basis sets, 6-31G*, 6-311G*, 6-31+G*, 6-311G*, and 6-311+g(2d,p). Basis-set dependence of those distances was examined. For the F⁻(SiF₄)_n cluster, a B3-LYP/6-31+G* basis was used, since diffuse functions(+) are indispensable to describe anionic systems.¹⁴ Electronic energies were calculated by Becke3LYP/6-311+G-(2df,2p) single-point calculations on the B3-LYP/6-31(+)+G* geometries. These combinations are recommended as accurate and practical methods.¹⁵ For F⁻(SiF₄)₁, the F⁻⋯SiF₄ bond energy was recalculated by QCISD(T)/6-311+G**/B3-LYP/6-31+G*. All the calculations were carried out using the GAUSSIAN 94 program,¹⁶ which was installed at the CONVEX SPP-1200/XA in the Information Processing Center, Nara University of Education.

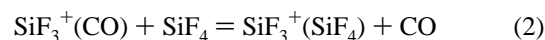
3. Experimental Results

3.1. Thermochemical Stability of SiF₃⁺(CO)_n. In the measurement of the clustering reaction 1,



an equilibrium between SiF₃⁺ and SiF₃CO⁺ could not be observed due to the rapid conversion of SiF₃⁺ into SiF₃CO⁺ up to the highest temperature measured, 740 K. This leads to the lower limit of the bond dissociation for SiF₃⁺⋯CO to be >35 kcal/mol. It was found that SiF₃⁺(SiF₄) started to be observed (the major ion was SiF₃CO⁺) when the ion source temperature was increased above ~490 K. This is due

to the occurrence of the displacement reaction 2 at the highertemperature region:



The equilibrium for reaction 2 was established above 490 K. It was confirmed that the equilibrium constants for reaction 2 were independent of the change of the ratio of the pressure of SiF₄ and CO, P[SiF₄]/P[CO]. Figure 1 shows the temperature dependence of the equilibrium constants for reaction 2 as the van't Hoff plots in the temperature range of 480–740 K. The straight van't Hoff plots lead to the determination of thermochemical data for reaction 2 to be $\Delta H^\circ = 4.0$ kcal/mol and $\Delta S^\circ = 8$ cal mol⁻¹ K⁻¹. That is, reaction 2 is endothermic by 4.0 kcal/mol. In our previous paper,⁷ the bond dissociation energy of SiF₃⁺⋯SiF₄ was estimated to be 37.7 kcal/mol. This value leads to the bond dissociation energy of SiF₃⁺⋯CO to be 37.7 + 4.0 = 41.6 kcal/mol. In Figure 1 the van't Hoff plots for reaction 1 with $n = 2$ are also displayed. The thermochemical data were determined to be $-\Delta H_{1,2}^\circ = 15.2$ kcal/mol and $-\Delta S_{1,2}^\circ = 26$ cal mol⁻¹ K⁻¹ (Table 1). Unfortunately, thermochemical values for $n \geq 3$ could not be obtained due to the serious charging of the ion source at lower temperature as was explained in the previous section.

The obtained bond energy of SiF₃⁺⋯CO (41.6 kcal/mol) is much larger than that of the isovalent CF₃⁺⋯CO, 16.0 kcal/mol.¹⁷ This indicates that SiF₃⁺ is a much stronger Lewis acid than CF₃⁺. The bond energies for CF₃⁺(CO)_n showed an irregular decrease between $n = 1$ and $n \geq 2$ (the bond energy for CF₃CO⁺⋯CO is only 6.3 kcal/mol). That is, the core ion

TABLE 1: Thermochemical Data, $-\Delta H_{n-1,n}^o$ (kcal/mol) and $-\Delta S_{n-1,n}^o$ (cal mol⁻¹ K⁻¹) for Reactions 1–5 Listed in the Text^{a,b,c}

	$n = 1$		$n = 2$	
	$-\Delta H_{n-1,n}^o$	$-\Delta S_{n-1,n}^o$	$-\Delta H_{n-1,n}^o$	$-\Delta S_{n-1,n}^o$
(1) SiF ₃ ⁺ (CO) _{n-1} + CO =	41.6		15.2	26
SiF ₃ ⁺ (CO) _n	[41.96]		[16.83]	
(3) SiF ₃ OH ₂ ⁺ (SiF ₄) _{n-1} +	9.6	15	7.7	19
SiF ₄ = SiF ₃ OH ₂ ⁺ (SiF ₄) _n	[8.67]		[8.63]	
(4) SiF ₄ H ⁺ (SiF ₄) _{n-1} +	18.9	24		
SiF ₄ = SiF ₄ H ⁺ (SiF ₄) _n	[21.12]		[3.16]	
(5) F ⁻ (SiF ₄) _{n-1} + SiF ₄ =			9.6	15
F ⁻ (SiF ₄) _n	[69.67]		[11.40]	
			ΔH^o	ΔS^o
(2) SiF ₃ ⁺ (CO) + SiF ₄ = SiF ₃ ⁺ (SiF ₄) + CO			4.0	8
			[5.66]	

^a In square brackets, theoretical data of B3-LYP/6-311+G(2df,2p) electronic energies and B3-LYP/6-31G* zero-point vibration energies (ZPEs) are shown. For $n = 1$ of reaction 5, [73.93] kcal/mol is calculated by QCISD(T)/6-311+G* electronic energies and the B3-LYP/6-31+G* ZPEs. ^b Experimental errors for ΔH^o and ΔS^o values are 0.3 kcal/mol and 3 cal mol⁻¹ K⁻¹, respectively. ^c Enthalpy changes in square brackets are theoretical energies.

in the cluster ion CF₃⁺(CO)_n is CF₃CO⁺ and the $n \geq 2$ CO ligands interact with the core ion electrostatically.¹⁷ Namely, the cluster ion can be represented as CF₃CO⁺(CO)_{n-1}. In contrast, the $n = 2$ bond energy for SiF₃⁺(CO)_n in Table 1 is as large as 15.2 kcal/mol. This suggests that the core ion in the cluster ion SiF₃⁺(CO)_n is SiF₃⁺(CO)₂ rather than SiF₃CO⁺. As will be mentioned in the theoretical section, the central SiF₃⁺ in SiF₃⁺(CO)₂ is sandwiched by two CO ligands equivalently. In the interaction with the Lewis-base ligand, the carbon atom in CF₃⁺ is apt to have the sp³ hybridization orbital whereas the silicon atom in SiF₃⁺ is apt to retain the sp² hybridization orbital. Regardless of positive or negative ions, such a flexibility of the silicon atom in the silicon compounds leads to symmetric structures and a variety of chemical reactivities (shown later).

3.2. Thermochemical Stability of SiF₃OH₂⁺(SiF₄)_n. In the present experimental system, the formation of the ion with $m/z = 103$ which is one mass unit lower than SiF₄⁺ was observed. The rate of the formation of this ion was apparently slower than those of the primary ions SiF_m⁺. This ion was assigned to SiF₃⁺·OH₂ because this ion became the major ion when a small amount of water vapor was added in the reagent gas. This ion may be formed either by the recombination reaction of SiF₃⁺ with water impurity or by the displacement reaction of the cluster ions of SiF₃⁺ with H₂O. In the formation of amorphous silicon by the plasma CVD, the SiF₃OH₂⁺ could become the major ion if the vacuum chamber is contaminated by some moisture. The measured thermochemical data for clustering reaction 3 are given in Table 1.



The rather small and nearly n -independent $-\Delta H_{n-1,n}^o$ values with $n = 1$ and 2 suggest that the protic two H atoms of the core ion SiF₃OH₂⁺ are the electrophilic sites for the interaction with two SiF₄ ligands despite the apparent silicon cation center, F₃Si⁺·OH₂.

3.3. Thermochemical Stability of SiF₄H⁺(SiF₄)_n. Shimizu and co-workers fabricated the micro- and crystal polysilicon

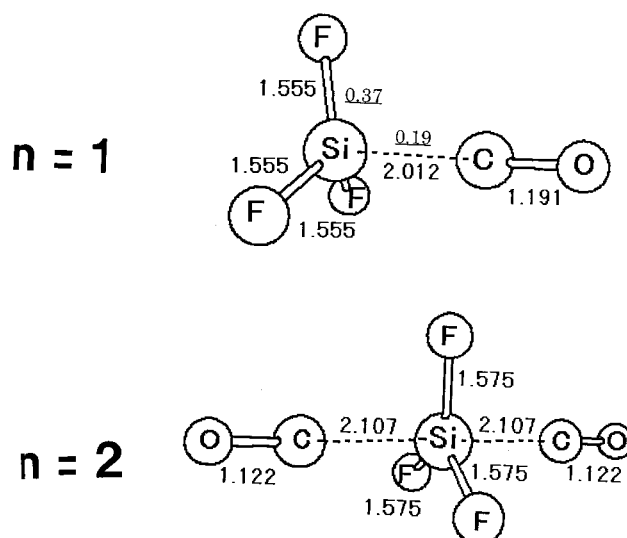
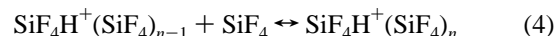


Figure 2. Geometries of SiF₃⁺(CO)_n optimized by B3-LYP/6-31G*. Distances are in angstrom, and those of free SiF₃⁺ and CO molecules are 1.539 Å (Si-F) and 1.13 Å (C-O), respectively. The SiF₃⁺(CO)₁ cluster is of C_{3v} point group and the SiF₃⁺(CO)₂ is of D_{3h} one. The underlined numbers denote off-diagonal atom-atom bonding populations.

by low temperature (≤ 360 °C) plasma-enhanced CVD using mixed gas of H₂ and SiF₄.⁸⁻¹⁰ So far, no plasma diagnosis has been made for the identification of the ionic species in these plasmas. In the present SiF₄/H₂ system, about equal abundances of SiF₃⁺ and SiF₄H⁺ ions as major ions were formed in addition to minor Si⁺ and SiF⁺ ions (about 10% of the former ions). Such ions accelerated in the sheath of the plasma may play important roles for the anisotropic etching of the fabricated silicon surface.

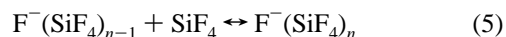
In our previous work, the bond energies of CH₅⁺·CH₄¹⁸ and CF₄H⁺·CF₄¹⁷ were determined to be 6.9 and 5.1 kcal/mol, respectively. We failed to measure the bond energy of SiH₅⁺·SiH₄ because we could not generate the SiH₅⁺ ion under any experimental conditions. To compare the nature of bonding for CF₄H⁺ and SiF₄H⁺ ions, the equilibrium for reaction 4 has been measured.



The thermochemical values obtained for $n = 1$ are given in Table 1. The data with $n \geq 2$ could not be obtained due to charging of the ion source.

The measured bond energy of SiF₄H⁺·SiF₄, 18.9 kcal/mol, is much larger than that of CF₄H⁺·CF₄ (6.9 kcal/mol). As will be mentioned later, the complex SiF₄H⁺·SiF₄ may be represented as the SiF₃⁺ (nearly D_{3h} symmetry) sandwiched by HF and SiF₄, i.e., F₃SiF⁺·SiF₃⁺·FH. Again, the vacant 3p_π orbital of the sp² hybridized silicon atom in the nearly planar core ion SiF₃⁺ accommodates the two ligands.

3.4. Thermochemical Stability of F⁻(SiF₄)_n. In the negative ion mode operation, no negative ions were detected when a few Torr of reagent He/SiF₄ gas was irradiated by 2 keV electrons. This is reasonable because the adiabatic electron affinity of SiF₄ is predicted to be negative.⁶ To observe the equilibria for reaction 5, about 0.1 Torr of NF₃ was added into the 3 Torr reagent He/SiF₄(95/5) gas through the stainless steel capillary.



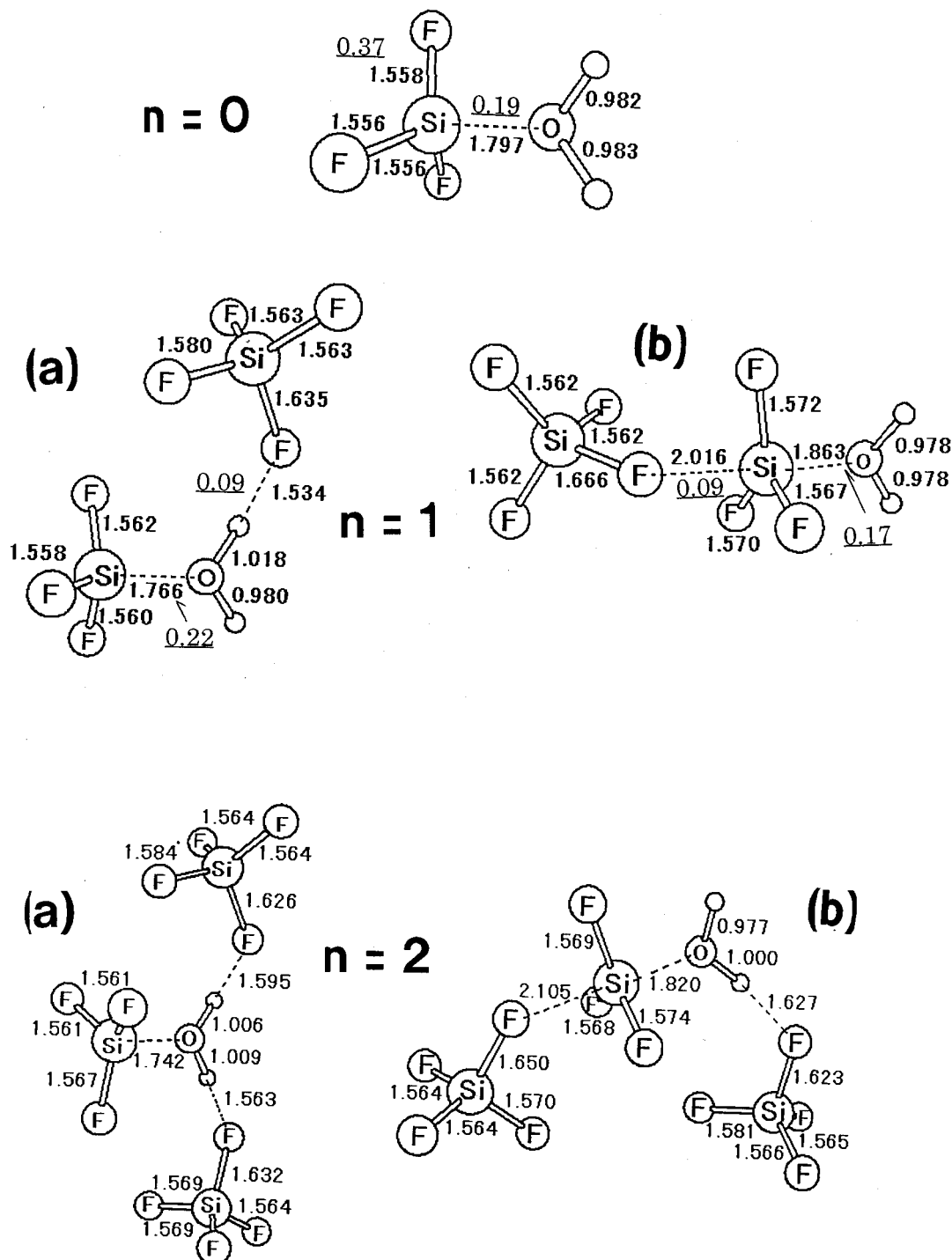


Figure 3. Geometries of $\text{SiF}_3\text{OH}_2^+(\text{SiF}_4)_n$. The (a) isomer of $n = 1$ is more stable than the (b) one by 1.25 kcal/mol (B3-LYP/6-311+G(2df,2p)/6-31G* ZPE). (a) is more stable than (b) by 6.49 kcal/mol in $n = 2$. Empty circles stand for hydrogen atoms.

Even at the highest temperature measured (740 K), equilibria with $n = 1$ could not be observed. That is, the F^- ions generated from NF_3 by electron capture were completely converted to SiF_5^- and no free F^- ions were observed after the electron pulse. This was reasonably expected because the bond energy of SiF_5^- (D_{3h} symmetry with the $^1A_1'$ ground state), $\text{SiF}_5^- \rightarrow \text{SiF}_4 + \text{F}^-$, is predicted to be 83 kcal/mol.⁶ The upper limit of the measurable bond energies using high-pressure mass spectrometry is, at most, 35–40 kcal/mol. The thermochemical data for reaction 5 with $n = 2$ were determined to be $-\Delta H_{0,2}^\circ = 9.6$ kcal/mol and $-\Delta S_{0,2}^\circ = 15$ cal mol⁻¹ K⁻¹ (Table 1). The steep decrease in the bond energies of $\text{F}^-(\text{SiF}_4)_n$ with $n = 1 \rightarrow 2$ suggests that the nature of bonding changes drastically from

covalent to electrostatic with $n = 1 \rightarrow 2$. This is reasonable because the negative charge is well dispersed in the core ion $[\text{F}\cdots\text{SiF}_3\cdots\text{F}]^-$.

4. Theoretical Results and Discussion

Figure 2 shows geometries of $\text{SiF}_3^+(\text{CO})_n$ ($n = 1$ and 2). These are similar to $\text{SiH}_3^+(\text{CO})_n$ ¹⁹ whose Si \cdots C distances are 2.02 Å ($n = 1$) and 2.23 Å ($n = 2$), respectively. The $3p_z$ atomic orbital of the silicon atom is coordinated to the lone-pair orbital of carbon monoxide. The Si–F antibonding character of LUMO of SiF_3^+ is reflected by elongation of the Si–F bond through charge acceptance.

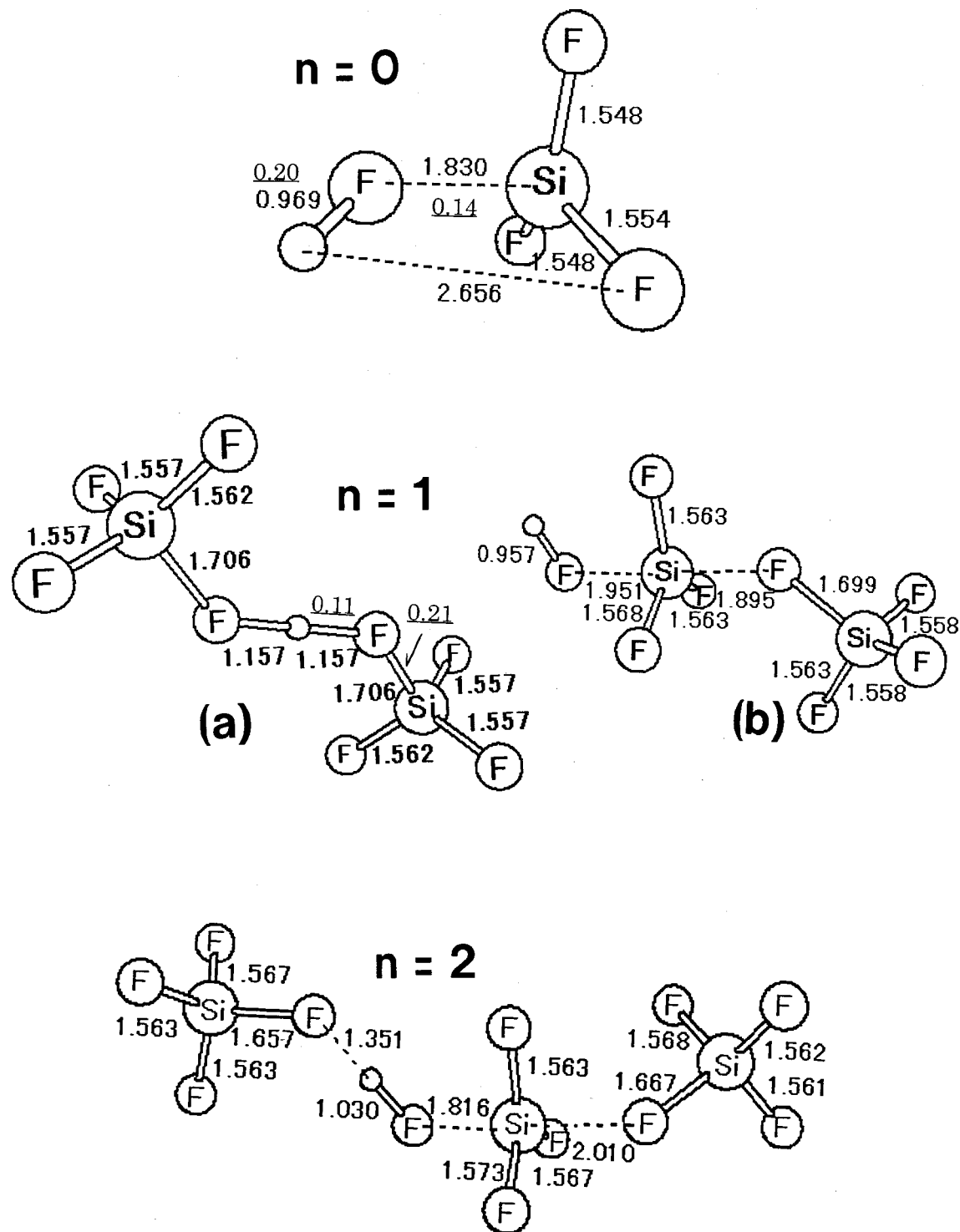
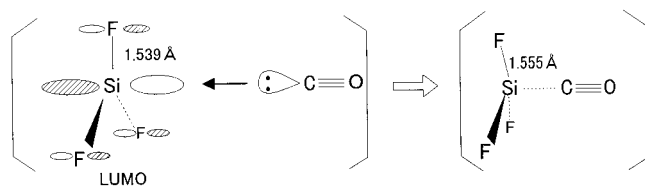
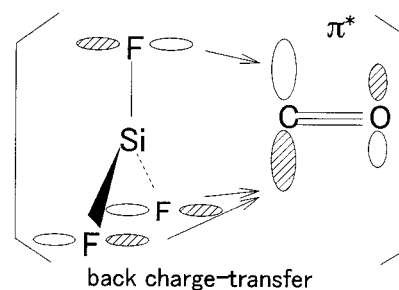


Figure 4. Geometries of SiF₄H⁺(SiF₄)_n. In *n* = 1, (a) is of C₂ point group and 8.41 kcal/mol more stable than (b).



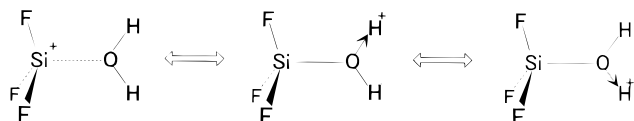
In Table 1, the computed energies are displayed in square brackets. The F₃Si⁺...CO bond energy is calculated to be [41.96] kcal/mol which is in excellent agreement with the present experimental value, 41.6 kcal/mol. The value is larger than that of H₃Si⁺...CO (= 34.27 kcal/mol by MP4/6-31G*)¹⁹ and that

of F₃C⁺...CO (= 16.0 kcal/mol, exptl).¹⁷ The following back charge-transfer strengthens the F₃Si⁺...CO interaction. As in



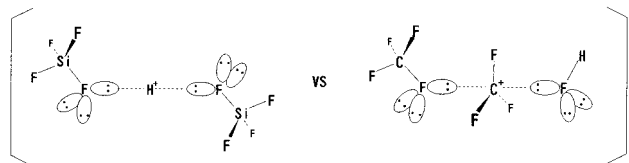
$\text{H}_3\text{Si}^+(\text{CO})_2$, the $\text{F}_3\text{Si}^+(\text{CO})_2$ geometry is of D_{3h} point group. The $\text{OC}-\text{SiF}_3^+\cdots\text{CO}$ bond energy is calculated to be [16.83] kcal/mol which is in good agreement with the present experimental one, 15.2 kcal/mol. These values are larger than those ([11.1] and 10.72 kcal/mol) of $\text{OC}-\text{H}_3\text{Si}^+\cdots\text{CO}^{19}$ owing to the above-mentioned back charge-transfer in $\text{F}_3\text{Si}^+(\text{CO})_2$. The atom-atom bond populations are attached to the $n = 1$ geometry as the underlined numbers. The $\text{Si}\cdots\text{C}$ population 0.19 is much smaller than that 0.36 of $\text{F}_3\text{Si}-\text{CH}_3$, which indicates that the $\text{Si}\cdots\text{CO}$ is a coordination bond rather than a covalent bond. Thus, the $n = 1$ cluster may be regarded as a strong Mulliken charge complex.

Figure 3 shows geometries of $\text{F}_3\text{SiOH}_2^+(\text{SiF}_4)_n$ clusters ($n = 0, 1$, and 2). In $n = 1$, two geometric isomers (a) and (b) were obtained. The $n = 1$ (b) is a model expected by the $\text{OC}\cdots\text{SiF}_3^+\cdots\text{CO}$ double coordination geometry in Figure 2. However, a hydrogen-bonded model, $n = 1$ (a), is more stable than $n = 1$ (b) by 1.25 kcal/mol. In $n = 0$, H_2O is bonded strongly to SiF_3^+ (bond energy = 69.41 kcal/mol), and $(\text{SiF}_3\text{OH}_2)^+$ is midway between $\text{SiF}_3^+(\text{H}_2\text{O})$ and $(\text{F}_3\text{SiOH})\text{H}^+$.



In fact, the O-H distances 0.982 and 0.983 Å are larger than that 0.967 Å in H_2O . The $\text{Si}\cdots\text{O}$ bond distance 1.797 Å in $n = 0$ is not so large relative to 1.624 Å in $\text{F}_3\text{Si}-\text{OH}$. The backside of $\text{F}_3\text{Si}^+\text{OH}_2$ loses the electrophilic ability. In $n = 2$, again, the hydrogen-bond coordination geometry (a) is more favorable than the mix-type (hydrogen bond and backside coordination) (b) by 6.49 kcal/mol. In Table 1, the computed bond energies [8.67] kcal/mol ($n = 1$) and [8.63] kcal/mol ($n = 2$) are in fair agreement with present experimental ones 9.6 and 7.7 kcal/mol, respectively.

In Figure 4, $\text{SiF}_4\text{H}^+(\text{SiF}_4)_n$ geometries ($n = 0, 1$, and 2) are shown. The $n = 0$ geometry is regarded as a complex between hydrogen fluoride and SiF_3^+ . This type of the complex was also obtained in the CF_4H^+ .¹⁷ But the charge dispersal in $\text{F}_3\text{Si}^+\cdots\text{FH}$ is more extended than that in $\text{F}_3\text{C}^+\cdots\text{HF}$. The $\text{Si}\cdots\text{F}$ distance, 1.830 Å, of $\text{F}_3\text{Si}^+\cdots\text{FH}$ is much shorter than the $\text{C}\cdots\text{F}$ one, 2.211 Å,¹⁷ in view of covalent-bond lengths $\text{Si}-\text{F} = 1.539$ Å in SiF_4 and $\text{C}-\text{F} = 1.302$ Å in CF_4 . That is, the protic character in SiF_4H^+ is larger than that in CF_4H^+ , and accordingly the following contrast of $n = 1$ has been obtained.



In fact, the $n = 1$ (a) hydrogen-bond geometry is more stable (by 8.41 kcal/mol) than the $n = 1$ (b) double coordination model. In $n = 2$, the second SiF_4 molecule is linked with $\text{SiF}_4\text{H}^+(\text{SiF}_4)_1$ by the backside coordination. In Table 1, the $n = 0 \rightarrow 1$ bond energy is large, 18.9 [21.12] kcal/mol owing to strong hydrogen bond formation. A large falloff of bond energies [21.12] \rightarrow [3.16] kcal/mol is shown as $n = 1 \rightarrow 2$. The backside coordination of $n = 2$ cannot get enough stability.

The influence of basis sets on the geometric results was examined. Five basis sets, 6-31G*, 6-311G*, 6-31+G*, 6-311+G*, and 6-311+G(2d,p), were adopted for B3LYP

TABLE 2: Basis-Set Dependence of Distances (Å) of Coordination Bonds in Cation Clusters

computational method	Si \cdots C distance in $\text{F}_3\text{Si}(\text{CO})_1$	Si \cdots O distance in $\text{F}_3\text{SiOH}_2^+$	F \cdots Si distance in $\text{H}^+(\text{SiF}_4)_1$
B3LYP/6-31G*	2.012 ^a	1.797 ^b	1.830 ^c
B3LYP/6-311G*	2.007	1.787	1.827
B3LYP/6-31+G*	2.016	1.797	1.833
B3LYP/6-311+G*	2.010	1.786	1.831
B3LYP/6-311+G(2d,p)	2.012	1.775	1.830

^a $n = 1$ in Figure 2. ^b $n = 0$ in Figure 3. ^c $n = 0$ in Figure 4.

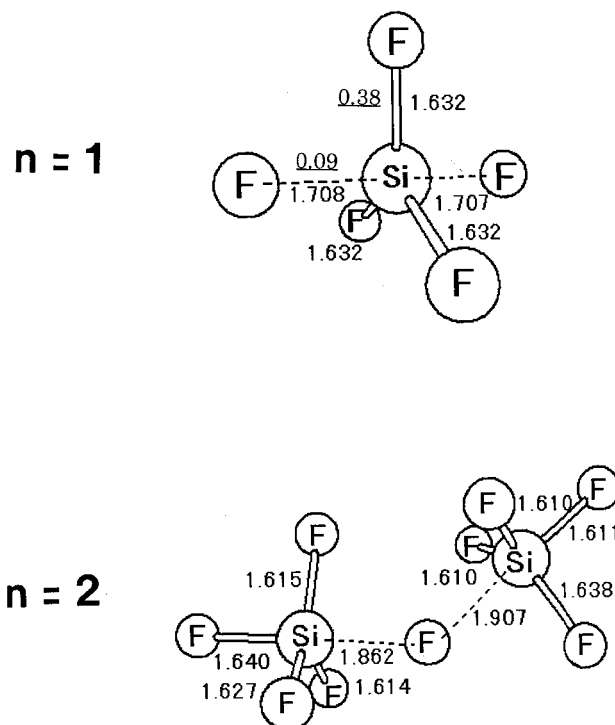
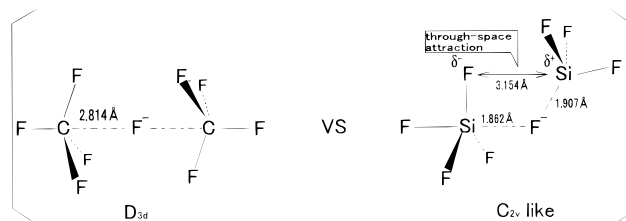


Figure 5. Geometries of $\text{F}^-(\text{SiF}_4)_n$.

calculations of $\text{F}_3\text{Si}(\text{CO})_1^+$, $\text{F}_3\text{SiOH}_2^+$, and $\text{H}^+(\text{SiF}_4)_1$. Table 2 shows Si \cdots C, Si \cdots O, and F \cdots Si distances in those species. They were found to be rather insensitive to the choice of basis sets, and the B3LYP/6-31G* geometry optimization used throughout this work seems to be reliable.

Figure 5 shows $\text{F}^-(\text{SiF}_4)_n$ geometries ($n = 1$ and 2). The $n = 1$ geometry has D_{3h} point group where two axial Si-F bonds are longer than three equatorial ones as in a valence isoelectronic species, PCl_5 . A contrast is observed between $\text{F}^-(\text{CF}_4)_1$ with C_{3v} point group²⁰ and $\text{F}^-(\text{SiF}_4)_1$ with D_{3h} point group.

For $n = 2$, there is another contrast.



The $\text{F}^-\cdots\text{Si}$ interaction is stronger than the $\text{F}^-\cdots\text{C}$ one, and the former leads to the $\text{Si}\cdots\text{F}\cdots\text{Si}$ bent (angle = 136.7°) geometry owing to a $\text{F}\cdots\text{Si}$ through-space attraction. In Table 1, the $\text{F}_4\text{Si}\cdots\text{F}^-$ bond energy is over 70 kcal/mol, which is enormously larger than 6.4 kcal/mol of $\text{F}_4\text{C}\cdots\text{F}^-$.¹⁷

In this work, various SiF_4 clusters have been examined. Hydrogen bonds (rather than coordination $\text{F}\cdots\text{Si}$ bonds) and

symmetric geometries are favored in SiF₄ clusters. Experimental energies were well reproduced by ab initio calculations. The nature of bonding in SiF₄ clusters is in sharp contrast with that in CF₄ clusters.

References and Notes

- (1) Schoolcraft, T. A.; Garrison, B. J. *J. Am. Chem. Soc.* **1991**, *113*, 8221.
- (2) Kickel, B. L.; Fisher, E. R.; Armentrout, P. B. *J. Phys. Chem.* **1993**, *97*, 10198.
- (3) Fisher, E. R.; Kickel, B. L.; Armentrout, P. B. *J. Phys. Chem.* **1993**, *97*, 10204.
- (4) Gutsev, G. L. *J. Chem. Phys.* **1993**, *99*, 3906.
- (5) Jacox, M. E.; Irikura, K. K.; Thompson, W. E. *J. Chem. Phys.* **1995**, *103*, 5308.
- (6) King, R. A.; Mastryukov, V. S.; Schaeffer, H. F., III. *J. Chem. Phys.* **1996**, *105*, 6880.
- (7) Hiraoka, K.; Nasu, M.; Minamitsu, A.; Shimizu, A.; Oomori, D.; Yamabe, S. *J. Phys. Chem.* **1999**, *103*, 568.
- (8) Ishihara, S.; He, D.; Shimidu, I. *Jpn. J. Appl. Phys.* **1994**, *33*, 51.
- (9) Akasaka, T.; He, D.; Miyamoto, Y.; Kitazawa, N.; Shimizu, I. *Thin Solid Films* **1997**, *296*, 2.
- (10) Kamiya, T.; Nakahara, K.; Ro, K.; Fortmann, C. M.; Shimizu, I. *Jpn. J. Appl. Phys.* **1999**, *38*, 5750.
- (11) Kebarle, P. In *Techniques for the Study of Ion-Molecule Reaction*; Farrar, J. M.; Saunders, W. H., Eds.; Wiley: New York, 1988.
- (12) Hiraoka, K. *J. Chem. Phys.* **1987**, *87*, 4048.
- (13) (a) Becke, A. D.; *J. Chem. Phys.* **1993**, *98*, 5648. (b) Becke, A. D. *Phys. Rev.* **1988**, *A38*, 3098. (c) Lee, C.; Yang, W.; Parr, R. G. *Phys. Rev.* **1988**, *B37*, 785. (d) Vosco, S. H.; Wilk, L.; Nusair, M. *Can. J. Phys.* **1980**, *58*, 1200.
- (14) Clark, T.; Chandrasekhar, J.; Spitznagel, G. W.; Schleyer, P. v. R. *J. Comput. Chem.* **1983**, *4*, 294.
- (15) Foresman, J. B.; Frisch, A. E. *Exploring Chemistry with Electronic Structure Methods*, 2nd ed.; Gaussian Inc.: Pittsburgh, PA, 1995; Chapter 7, p 158.
- (16) Frisch, M. J.; Trucks, G. W.; Schlegel, H. B.; Gill, P. M. W.; Johnson, B. G.; Robb, M. A.; Cheeseman, J. R.; Keith, T. A.; Petersson, G. A.; Montgomery, J. A.; Raghavachari, K.; Al-Laham, M.; Zakrzewski, V. G.; Ortiz, J. V.; Foreman, J. B.; Cioslowski, J.; Stefanov, B. B.; Nanayakkara, A.; Challacombe, M.; Peng, C. Y.; Ayala, P. Y.; Chen, W.; Wong, M. W.; Andres, J. L.; Replogle, E. S.; Gomperts, R.; Martin, R. L.; Fox, D. J.; Binkley, J. S.; Defrees, D. J.; Baker, J.; Stewart, J. P.; Head-Gordon, M.; Gonzalez, C.; Pople, J. A. *Gaussian 94 (Revision A.1)*; Gaussian, Inc.: Pittsburgh, PA, 1995.
- (17) Hiraoka, K.; Nasu, M.; Ignacio, E. W.; Yamabe, S. *J. Phys. Chem.* **1996**, *100*, 5245.
- (18) Hiraoka, K.; Mori, T. *Chem. Phys. Lett.* **1989**, *161*, 111.
- (19) Hiraoka, K.; Katsuragawa, J.; Sugiyama, T.; Minamitsu, A.; Yamabe, S.; Kouno, H. *Chem. Phys. Lett.* **1997**, *271*, 302.
- (20) Hiraoka, K.; Nasu, M.; Fujimaki, S.; Ignacio, E. W.; Yamabe, S. *Chem. Phys. Lett.* **1995**, *245*, 14.